In situ assembly of linked geometrically coupled microdevices

T. Sawetzki[a], S. Rahmouni[a], C. Bechinger[a,b], and D. W. M. Marr[c,1]

[a]Physikalisches Institut, Universität Stuttgart, Pfaffenwaldring 57, 70550 Stuttgart, Germany; [b]Max-Planck-Institut für Metallforschung, Heisenbergstrasse 3, 70569 Stuttgart, Germany; and [c]Chemical Engineering Department, Colorado School of Mines, Golden, CO 80401

Complex systems require their distinct components to function in a dynamic, integrated, and cooperative fashion. To accomplish this in current microfluidic networks, individual valves are often switched and pumps separately powered by using macroscopic methods such as applied external pressure. Direct manipulation and control at the single-device level, however, limits scalability, restricts portability, and hinders the development of massively parallel architectures that would take best advantage of microscale systems. In this article, we demonstrate that local geometry combined with a simple global field can not only reversibly drive component assembly but also power distinct devices in a parallel, locally uncoupled, and integrated fashion. By employing this single approach, we assemble and demonstrate the operation of check valves, mixers, and pistons within specially designed microfluidic environments. In addition, we show that by linking these individual components together, more complex devices such as pumps can be both fabricated and powered in situ.

colloids | microfluidics | micromachines

O ver the past decade, there has been significant interest in microfluidic technology; however, its impact has and will remain limited without widespread use (1). To broaden application into areas such as the typical laboratory for research application or point of care for biomedical analysis, there is a need for simplified devices that retain complex function. One significant hurdle to this realization is the in-place fabrication and integration of individual fluidic microcomponents. Small pieces simply cannot be easily handled or connected in a manner comparable with macroscale device fabrication. To overcome this, nature has chosen self-assembly (2), a process where intermolecular forces drive component joining; however, replicating this approach requires the difficult synthesis of molecular-scale parts with desired specific interactions. In recent efforts within larger-scale microfluidic systems, other authors have used in situ optical-based fabrication (3, 4) and flow-driven assembly (5) to create active and predesigned microstructures. In a smaller-scale method for device self-assembly that avoids the need for fabrication of individual components, we instead employ micron-size spherical colloidal particles as building blocks (6) with interactions that are well-modeled and readily altered through modification of surface chemistry or solution composition (7, 8). Most importantly for this work, their interactions can be dynamically and dramatically changed through application of an external field (9, 10), allowing device assembly and operation within specially designed confining environments for microscale "ship-in-a-bottle" construction.

Specifically, we employ magnetic fields for device construction because these can be readily generated and, because of their simplicity, are often used in bioassaying applications for separations of targeted proteins or cells (11–14). In this technique, colloidal particles that become strongly dipolar in the presence of a magnetic field (paramagnetic) are used and surface-modified with some targeting moiety. By applying magnetic fields within confining 2-dimensional microfluidic channels and

other geometries, the dipolar interactions can be carefully tuned from strongly attractive to strongly repulsive. We have previously shown that this fine control over interparticle forces can be used to create colloidal assemblies within microchannels after they have been introduced as a simple aqueous dispersion (15). Once individual components are fabricated in place, however, the ability to power and switch them is necessary. Analogous to wireless radio-frequency fields (16), magnetic fields can be used to transfer energy across length scales without direct contact, and we use these to provide the necessary energy for device function. In this method, a dynamic modulation of the applied field can be used to effectively "plug in" a microscale device and overcome the significant hurdle of interfacing between macro and micro worlds. One advantage of this approach is that it is inherently parallel—once a single device is powered, all devices within the field are simultaneously actuated.

High parallelization of indistinguishable parts operating identically limits potential function, however. With a global field used for assembling and powering multiple components, distinct device function must somehow be achieved in a local fashion. We demonstrate here a geometric approach where microdevice size and shape and confining microenvironment can be directly coupled to obtain a specific and independent component function. To highlight the flexibility of this method, we use a single bulk field to assemble and operate a set of the most common devices including valves, mixers, and pumps within their functioning microenvironments. Although, certainly, a significant number of other active microfluidic flow control techniques (17, 18) have been demonstrated elsewhere, in general, these are difficult to scale because of the nature of their actuation and integration methods.

Results and Discussion

Here, we describe our experiments with 3 devices, each designed to highlight a particular aspect of our approach: first, that assembly can be performed in confined geometries; second, that the approach can be used to power devices once fabricated; and third, that devices can be linked, and confining structure can play an important role in both device assembly and function. Finally, and in the context of this last device, we discuss the assembly process in some detail.

In-Place Assembly—The Check Valve. Assembly of pieces within enclosed geometries is necessary for those devices that require components larger than their inlets and outlets. One device that clearly demonstrates the utility of in situ construction is the
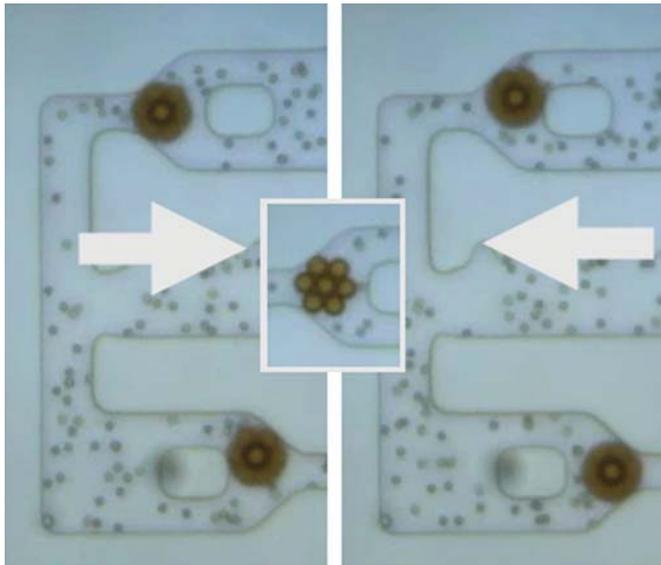
Fig. 1. Check valve position as a function of applied flow. *Inset* shows colloidal assembly composed of 4.5-μm particles, when the field is turned off. Note that 1.5-μm particles are used here as flow tracers.

Fig. 2. Measured lateral concentration profiles of 0.76-μm tracer particles at positions down the channel fit to Eq. **1** (photo upper right). The applied field case (photo lower left) with good mixing and an assembly rotation rate of $\approx$10 Hz. Channel width at measurement start is 100 μm (horizontal lines).

check valve, a fluidic rectifier where flow is allowed in one direction but not the other. To fabricate such a device at the microscale, individual components must be brought within the valve chamber and fused together in place. With the paramagnetic colloidal particles we employ in these studies, thin microfluidic channels provide a planar, pseudo 2D environment. As shown in Fig. 1, for check valve function, the confining geometry is chosen such that individual component particles can flow in and out of all connecting channels. With application of the bulk magnetic field, however, magnetic dipoles strongly attract, driving stable device assembly into a compact, lowest-energy morphology. As can be readily seen here, the 7-particle clusters formed are too large to pass either through the valve outlet or inlet. Of important note is the assembly process is a reversible one; as the field is switched off, the clusters will disassemble, turning off device function if desired. One significant advantage of the colloids we use here is that they are readily available with a variety of surface functionalities, including reactive groups that can be used for irreversible assembly binding (19) if continued device operation is useful after field switch-off. And although only 2 of these valves are shown, their construction could be performed in a parallel fashion because of the global nature of the driving field.

In Fig. 1, function of the individual valves is demonstrated by fluid movement in the center channel; flow to the right closes the top valve and opens the bottom—flow to the left closes the bottom valve and opens the top. Although the single surrounding field has been used for assembly of both, it is important to note that individual valve action is uncoupled; flow blocks 1 channel but simultaneously opens the other. Efficiency of the valves is influenced by multiple factors. Because the colloidal building blocks are spherical, they do not completely block flow V, a potential issue for some applications that cubic, space-filling colloidal building blocks (20) with embedded functionality could solve. In addition and because of the dynamic nature of the assembly method, field rotation leads to a net torque on the colloidal assembly. Apparent in the accompanying Movie S1, this rotation induces a local flow that prevents a tight seal with the channels they are designed to block with a measured value of $V_o/(V_o + V_c) = 64\%$.
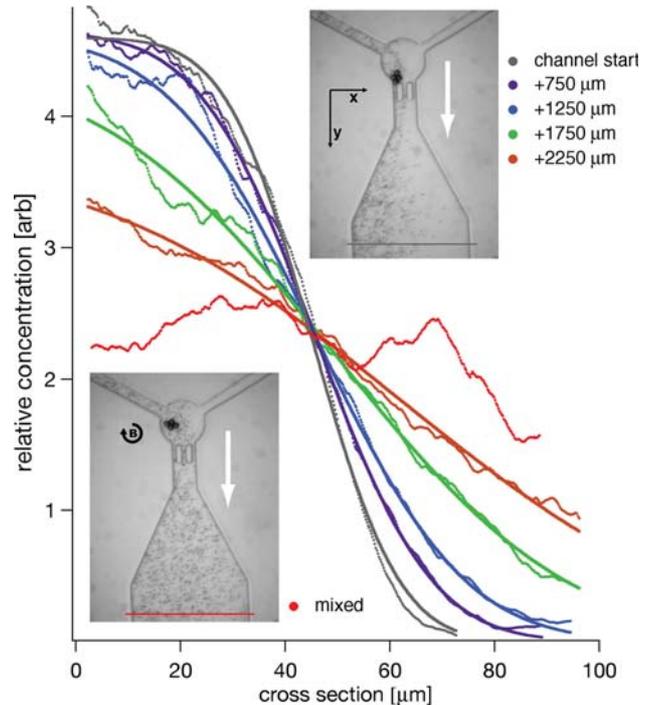
Power Across Length Scales—Mixing. Rapid assembled-cluster rotation may be a disadvantage for this particular valve design, but associated fluid movement can be useful for other applications. It is well-known and a significant area of research in microfluidics that mixing in microscale geometries is difficult because of the laminar nature of the fluid flows, the associated lack of turbulence, and the resulting reliance on diffusion (21, 22). One design that has been used to mix in relatively large microfluidic devices is to use multilayer soft lithography to create pumps and valves and mix fluids by circulating them within a circular channel (23), an approach that has been used, for example, in screening for protein crystallization (24). This technique, however, relies on the supporting pressurization equipment associated with operating many of these pumps simultaneously that limits very high-level parallelization.

Shown in Fig. 2 is an active mixer created through the assembly of small colloidal building blocks in a confining geometry in a manner similar to those used for the check valves. In this system, 2 separate streams, one an aqueous colloidal solution and the other without colloids, are brought together at a mixing junction before expansion into a standard square channel. To demonstrate the utility here, we use a relatively slow-diffusing tracer consisting of nonmagnetic 0.76-μm polystyrene particles. This represents a good system because lateral concentration profiles can be directly determined by particle counting and not inferred from a bulk measurement. Without magnetic field application, lateral concentration profiles were measured (Fig. 2) at the channel start and at distances significantly down the channel length (data not shown). Here, the curves of relative tracer concentration were fit to the simple solution for 1-dimensional diffusion (25) given a step concentration initial condition:

$$C(x, t) = \frac{C_0}{2} \, erfc\left(\frac{x}{\sqrt{4Dt}}\right) = \frac{C_0}{2} \, erfc\left(\frac{x}{\sqrt{4Dy/v}}\right), \qquad [\mathbf{1}]$$

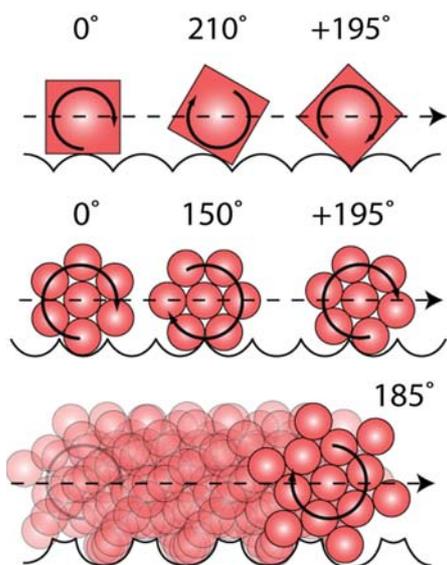**Fig. 3.** A square translates along a series of inverted catenaries, the particle clusters along a series of inverted cycloids (28).

Fig. 4. Coupled devices can be used to create more complex systems. (*A*) Pumping performed by a colloidal assembly piston using 4.5-μm particles as building blocks. (*B*) Pumped volume V (as measured in the boxed region) in channels with open (V_o, red) and closed (V_c, black) valves as a function of the pinion rotation frequency f. Measured check valve efficiency, independent of the rotation frequency f, is shown in the *Inset*.

with C_0 the initial tracer concentration, D the diffusion coefficient, x the lateral position, y the distance down the channel, and v the fluid velocity. Using the measured value of $v = 3.6$ μm/s, we fit the unmixed concentration profiles (Fig. 2) and find $D = 0.73$ μm^2/s, in good agreement with a value of 0.64 μm^2/s based on the particle radius and predicted from the Stokes–Einstein relation. Upon field actuation and rotation of the assembled cluster at $\approx$10 Hz, efficient mixing is readily observed in the region directly after the chamber. Quantifying the resulting concentration profile and using the diffusion values determined from the unmixed case, we predict, using Eq. **1**, that channel lengths >15 cm or times >10 h would be required to achieve a comparable level of tracer dispersion via diffusion alone.

Coupling Function to Local Geometry—Pumping. The assembled mixer clearly demonstrates that a global field can be used to dynamically control microsystems and transport power across length scales to drive a microscale device. As is well known for such systems, viscous effects dominate over inertial effects, giving rise to the laminar flow characteristics; however, we see from these studies that the magnetic forces that arise from the applied field can be significant. To quantify their relative strength we use the Mason (Mn) number (26), where

$$\text{Mn}^{-1} = \frac{\mu_0 M^2}{32\eta\omega v_0^3} = \frac{\text{magnetic forces}}{\text{viscous forces}}. \qquad [2]$$

For the rapidly rotating clusters of Fig. 1 composed of 4.5-μm particles (of volume $= v_0$) we estimate rotation rates of $\omega \approx 10$ s^{-1}. Using literature values for the magnetization M (27) at the low applied field strengths of $\approx$5 mT, where these experiments were conducted, we find $\text{Mn}^{-1} \approx 1,000$, emphasizing the strength of magnetic forces under these conditions. Such a clear dominance over fluid forces at these scales suggests that significant additional functionality is available with a modified approach.

To take advantage of this for useful microscale device operation, we need to harness assembly rotation in a manner that efficiently extracts rotational torque and imparts this to useful force propagation in desired directions. To do this, we employ a rack-and-pinion arrangement commonly associated with automotive steering mechanisms that couples pinion rotation to translation along the teeth of the complementary rack. The
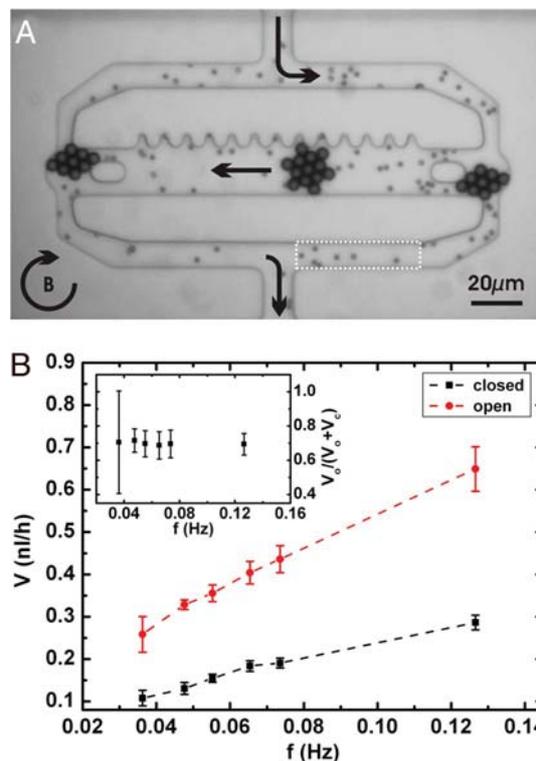
general concept is illustrated in Fig. 3, where a rotation of a square "wheel" leads to a smooth translation along a "road" composed of a series of truncated catenaries where $y = -\cosh(x)$ and the angle at which these catenaries meet corresponds to the interior angle of the square wheel (28). Mathematical solutions for the roads corresponding to wheels of arbitrary structure can also be generated and correspond to inverted cycloids for wheels constructed from assembled spheres; however, these have sharper profiles, features that replicate poorly during the soft lithography process at the necessary resolutions corresponding to the colloidal particles we employ here.

To demonstrate this approach, we integrate a microfluidic wall "rack" of slightly smoother structure than theoretically desired and a colloidal assembly "pinion" to create a piston capable of forcefully pushing fluid down a microfluidic channel. Although other designs are feasible, the rack in Fig. 4 is of finite length, requiring a reverse of the device rotation for continuous operation. To fix net system pumping in 1 direction as the field is switched between clockwise and counterclockwise rotation, we integrate the piston with active check valves composed once again of field-assembled colloidal particles. Here, a different geometry and diamond-shape structure was chosen to prevent assembly rotation and simplify design, with only 1 valve required at each device end. Available as Movie S2, real-time video of device actuation clearly demonstrates the parallel operation of multiple devices, the linked function of these devices, and the effectiveness of this approach. With the addition once again of nonparamagnetic tracer particles for flow visualization, we obtain at our low field strength flow rates of on the order of 1 nL/hr within the channel. Here, we see that the net flow is proportional to the rotation rate of the pinion, results that

demonstrate the strong coupling between field-induced rotation and colloidal assembly translation and function.

Here, it should be noted that, if the magnetic field is switched off, clusters fully disassemble and particles diffuse away by means of Brownian motion. Perhaps one of the most interesting observations of the behavior of these devices is their stability; once assembled they are, if not in their absolute ground state, in an extremely stable local minimum. This is due to a favoring of specific cluster shape with microfluidic wall interaction and the potential barrier that a particle must overcome to be translated into another position at the cluster exterior. Based on the magnetic dipole interaction and by comparing the number of nearest and next-nearest neighbors, we estimate that the cogwheel is energetically 12% above the ground state. To achieve lower energy configurations, however, an outer cogwheel particle would have to cross a barrier of ≈32% of the absolute potential well depth, and the diamond-shaped cluster tip would have to overcome 40% of its initial potential energy. This ability to strongly stabilize assemblies that are not necessarily in their energetic ground states through dynamic coupling to local geometry offers a greater variety of available components for microscale device development.

Conclusions

Microdevice fabrication and actuation using reversibly assembling colloidal systems and bulk magnetic fields provides a number of significant advantages over macroscopic techniques. The ability to easily and without direct contact link external energy sources to microscopic operation by local geometry coupling, without the loss of discrete device function, provides a promising route to practical and portable microsystem fabrication and operation. With the potential for massive parallelization, complex devices can clearly be assembled from simple, controllable, and modifiable building blocks within tightly confining microgeometries that influence the shape of the contained assembly by favoring the formation of dynamically stable clusters. The significant flexibility of this single technique has been demonstrated by the in situ powering and integration of multiple microfluidic devices including valves, mixers, and pumps. Although these results were obtained with associated instrumentation that is certainly macroscopic in size and not amenable to portable applications, the actual magnetic fields used were relatively small and could instead be generated with significantly smaller hardware (29, 30). Also, the components were assembled at microscopic sizes; however, the physics associated with magnetic-field based manipulation are scalable to smaller dimensions. Resolution in fabricating the surrounding matrices instead plays a significant role, and methods other than the soft lithography (31) used here, including those for glass or silicon, could
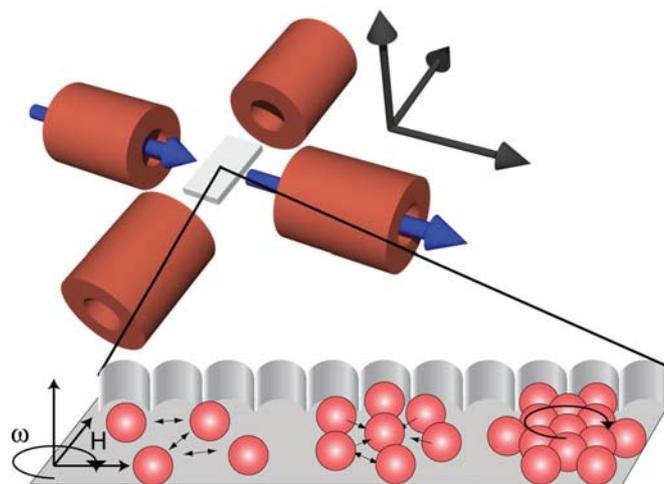

Fig. 5. A rotating magnetic field generated externally to the microfluidic device leads to attraction between individual particles in the sample plane and exerts a net torque on particle clusters once assembled.

be used instead because device function is not limited to elastic channel structures.

Materials and Methods

The microfluidic systems were assembled in polydimethylsiloxane (PDMS) by using standard soft-lithography techniques (32). The channels created by using this approach were planar and fabricated such that channel height was typically little more than the particle diameter. For our investigations, Dyna-beads (www.dynalbiotech.com) of diameter 4.5 μm were used; these readily available particles are superparamagnetic because of the presence of Fe_2O_3 and therefore exhibit magnetic properties only in the presence of a magnetic field. To create the magnetic fields, 4 coils of 25-mm diameter with 1,000 windings were placed pairwise around the device along the axes of the sample plane. Through these coils, currents between ≈1 and 3 A were applied in an offset and sinusoidally varying fashion at ≈100 Hz, each with 90° phase shift to its neighbors, resulting in ≈5 mT to induce both particle attraction and assembly rotation (33) within the microfluidic system (see Fig. 5). The coils were placed far enough apart that microfluidic devices ≈4 cm in diameter could easily be studied. In this setup, an optical trap was included for ease of particle manipulation and to control the number of paramagnetic colloids within confining environments. For tracer diffusion studies, 0.76-μm polystyrene particles (DS03R; Bangs) were used at low concentration; by using image processing (IPS; Visiometrics), these were individually counted and converted to normalized concentration for analysis.

1. Whitesides GM (2006) The origins and the future of microfluidics. *Nature* 442:368–373.
2. Whitesides GM, Grzybowski B (2002) Self-assembly at all scales. *Science* 295:2418–2421.
3. Kim D, Beebe DJ (2007) Hydrogel-based reconfigurable components for microfluidic devices. *Lab Chip* 7:193–198.
4. Pregibon DC, Toner M, Doyle PS (2007) Multifunctional encoded particles for high-throughput biomolecule analysis. *Science* 315:1393–1396.
5. Chung SE, Park W, Shin S, Lee SA, Kwon S (2008) Guided and fluidic self-assembly of microstructures using railed microfluidic channels. *Nat Mater* 7:581–587.
6. Glotzer SC, Solomon MJ (2007) Anisotropy of building blocks and their assembly into complex structures. *Nat Mater* 6:557–562.
7. Russel WB, Saville DA, Schowalter WR (1989) *Colloidal Dispersions* (Cambridge Univ Press, Cambridge, UK).
8. Belloni L (2000) Colloidal interactions. *J Phys Condens Matter* 12:R549–R587.
9. Gong T, Marr DWM (2001) Electrically switchable colloidal ordering in confined geometries. *Langmuir* 17:2301–2304.
10. Löwen H, *et al.* (2005) Colloidal layers in magnetic fields and under shear flow. *J Phys Condens Matter* 17:S3379–S3386.
11. Kim KS, Park JK (2005) Magnetic force-based multiplexed immunoassay using superparamagnetic nanoparticles in microfluidic channel. *Lab Chip* 5:657–664.
12. Tondra M, *et al.* (2001) Design of integrated microfluidic device for sorting magnetic beads in biological assays. *IEEE Transact Magnet* 37:2621–2623.
13. Inglis DW, Riehn R, Austin RH, Sturm JC (2004) Continuous microfluidic immunomagnetic cell separation. *Appl Phys Lett* 85:5093–5095.
14. Pamme N, Wilhelm C (2006) Continuous sorting of magnetic cells via on-chip free-flow magnetophoresis. *Lab Chip* 6:974–980.
15. Bleil S, Marr DWM, Bechinger C (2006) Field mediated self assembly and actuation of highly parallel microfluidic devices. *Appl Phys Lett* 88:263515.
16. Ye H, *et al.* (2007) Remote radio-frequency controlled nanoliter chemistry and chemical delivery on substrates. *Angew Chem Int Ed* 46:4991–4994.
17. Laser DJ, Santiago JG (2004) A review of micropumps. *J Micromech Microeng* 14:R35–R64.
18. Melin J, Quake SR (2007) Microfluidic large scale integration: The evolution of design rules for biological automation. *Annu Rev Biophys Biomol Struct* 36:213–231.
19. Biswal SL, Gast AP (2004) Micromixing with linked chains of paramagnetic particles. *Anal Chem* 76:6448–6455.
20. Panda P, *et al.* (2008) Stop-flow lithography to generate cell-laden microgel particles. *Lab Chip* 8.
21. Ottino JM, Wiggins S (2004) Introduction: Mixing in microfluidics. *Phil Trans R Soc London Ser A* 362:923–935.
22. Rothstein D, Henry E, Gollub JP (1999) Persistent patterns in transient chaotic fluid mixing. *Nature* 401:770–772.
23. Chou HP, Unger MA, Quake SR (2001) A microfabricated rotary pump. *Biomed Microdevices* 3:323–330.

24. Hansen CL, Sommer MOA, Quake SR (2004) Systematic investigation of protein phase behavior with a microfluidic formulator. *Proc Natl Acad Sci USA* 101:14431–14436.
25. Crank J (1975) *The Mathematics of Diffusion* (Oxford Univ Press, Oxford).
26. Biswal SL, Gast AP (2004) Rotational dynamics of semiflexible paramagnetic particle chains. *Phys Rev E* 69:041406.
27. Blickle V, Babic D, Bechinger C (2005) Evanescent light scattering with magnetic colloids. *Appl Phys Lett* 87:101102.
28. Hall L, Wagon S (1992) Roads and wheels. *Math Magazine* 65:283–301.
29. Ehrmann K, *et al.* (2007) Microfabricated solenoids and Helmholtz coils for NMR spectroscopy of mammalian cells. *Lab Chip* 7:373–380.
30. Lee H, Liu Y, Ham D, Westervelt RM (2007) Integrated cell manipulation system—CMOS/microfluidic hybrid. *Lab Chip* 7:331–337.
31. Whitesides GM, Stroock AD (2001) Flexible methods for microfluidics. *Phys Today* 54:42–48.
32. Xia Y, Whitesides GM (1998) Soft lithography. *Annu Rev Mater Sci* 28:153–184.
33. Tierno P, Muruganathan R, Fischer TM (2007) Viscoelasticity of dynamically self-assembled paramagnetic colloidal clusters. *Phys Rev Lett* 98:028301.